REPORT DOCUMENTATION PAGE

Form Approved
OMB No. 0704-0188

1. REPORT DATE (DD-MM-YYYY)	2. REPORT TYPE	3. DATES COVERED (From - To)
16-01-2003	Technical Paper	

4. TITLE AND SUBTITLE

Propellant Losses Because of Particulate Emission in a Pulsed Plasma Thruster

5a. CONTRACT NUMBER

5b. GRANT NUMBER

5c. PROGRAM ELEMENT NUMBER

6. AUTHOR(S)

Gregory G. Spanjers, Jason S. Lotspeich, Keith A. McFall, Ronald A. Spores

5d. PROJECT NUMBER
1011

5e. TASK NUMBER
0011

5f. WORK UNIT NUMBER

7. PERFORMING ORGANIZATION NAME(S) AND ADDRESS(ES)

Air Force Research Laboratory (AFMC)
AFRL/PRSS
1 Ara Drive.
Edwards AFB, CA 93524-7013

8. PERFORMING ORGANIZATION REPORT NUMBER

AFRL-PR-ED-TP-2003-011

9. SPONSORING / MONITORING AGENCY NAME(S) AND ADDRESS(ES)

Air Force Research Laboratory (AFMC)
AFRL/PRS
5 Pollux Drive
Edwards AFB CA 93524-7048

10. SPONSOR/MONITOR'S ACRONYM(S)

11. SPONSOR/MONITOR'S NUMBER(S)
AFRL-PR-ED-TP-2003-011

12. DISTRIBUTION / AVAILABILITY STATEMENT

Approved for public release; distribution unlimited.

13. SUPPLEMENTARY NOTES

14. ABSTRACT

20030227 158

15. SUBJECT TERMS

16. SECURITY CLASSIFICATION OF:			17. LIMITATION OF ABSTRACT	18. NUMBER OF PAGES	19a. NAME OF RESPONSIBLE PERSON
a. REPORT	b. ABSTRACT	c. THIS PAGE			Leilani Richardson
Unclassified	Unclassified	Unclassified	A		19b. TELEPHONE NUMBER (include area code) (661) 275-5015

DTS

MEMORANDUM FOR PRS (In-House Publication)

FROM: PROI (STINFO) 16 Jan 2003

SUBJECT: Authorization for Release of Technical Information, Control Number: **AFRL-PR-ED-TP-2003-011** Gregory G. Spanjers; Jason S. Lotspeich; Keith A. McFall; Ronald A. Spores, "Propellant Losses Because of Particulate Emission in a Pulsed Plasma Thruster"

Journal of Propulsion and Power **(Statement A)**
(July-Aug 1998 issue)

JOURNAL OF PROPULSION AND POWER
Vol. 14, No. 4, July–August 1998

Propellant Losses Because of Particulate Emission in a Pulsed Plasma Thruster

Gregory G. Spanjers,* Jason S. Lotspeich,† Keith A. McFall,† and Ronald A. Spores‡
U.S. Air Force Research Laboratory, Edwards Air Force Base, California 93524-7190

Propellant inefficiency material in particulate form is characterized in a laboratory pulsed plasma thruster (PPT) operating at 1 Hz with a 20-J discharge energy (20 W). Exhaust deposits are collected and analyzed using a combination of a scanning electron microscope with energy dispersive x-ray analysis and microscopic imaging. Teflon® particulates are observed with characteristic diameters ranging from over 100 μm down to less than 1 μm. Estimates show that the particulate emission consumes 40 ± 3% of total propellant mass while contributing less than 1% to the total thrust. If PPT modifications can be developed that eliminate this propellant loss mechanism, without affecting the PPT thrust, the potential exists to increase PPT efficiency by a factor of 1.7.

Nomenclature

f = discharge frequency
M = total propellant consumed in experimental run of N discharges
m = propellent consumed per discharge
N = number of discharges in experiment
P = thruster power
T = thrust
η = thrust efficiency

I. Introduction

THE pulsed plasma thruster (PPT)[1] is an attractive propulsion option for small power-limited satellites. The PPT, shown schematically in Fig. 1, operates at low power levels (<100 W) by charging an energy-storage capacitor on a long time scale (1 s), and then discharging on a short time scale (10 μs) at high instantaneous power. High reliability is achieved through the use of a solid propellant (typically Teflon®), which eliminates the complexity and dry mass associated with liquid or gaseous propellants. The only moving part on the PPT is a spring that passively feeds the propellant into the discharge chamber. The solid propellant is converted to vapor and partially ionized by a surface discharge across the propellant face. Acceleration is accomplished by a combination of thermal and electromagnetic forces to create usable thrust. The inherent engineering advantages of the PPT design have enabled the thruster to complete several space missions over the past 30 years with no failures.[1-3] Unfortunately, the excellent engineering characteristics of the PPT are coupled with poor performance characteristics. Flight-qualified designs[4] have achieved thrust efficiencies ($\eta = T^2/2fmP$) below 8%. The low thrust efficiency is attributable to both a low energy efficiency and a low propellant efficiency.[5,6] Previous measurements[5] have shown that neutral gas vaporizing from the propellant face long after the current discharge is a significant factor in the low propellant efficiency.

In the present work a second mechanism, particulate emission, is identified as a significant contributor to the low propellant efficiency. Broadband emission indicative of particulates is observed emitting from a laboratory PPT long after the current pulse. Microscope images of exhaust deposits collected on witness plates shows particulates in agreement with the emission measurements. Surface analysis of the witness plates using a scanning electron microscope with energy dispersive x-ray microanalysis (SEM/EDAX) supports the conclusion that the particulates originate from the Teflon propellant, as opposed to originating from the steel electrodes. The propellant mass expended in particulate form is estimated to be 40 ± 3% of the total mass ablated during the PPT discharge. Based on estimates of the particulate velocity from the broadband emission measurements, the particulate contribution to the total PPT thrust is less than 1%. Therefore, PPT modifications that eliminate the particulate emission may significantly reduce the propellant consumption with minimal decrease in thrust. In the optimal case, the PPT thrust efficiency could be increased by a factor of 1.7. For a Lincoln Experimental Satellite (LES) 8/9 PPT[4] this would increase the thrust efficiency from 7.9 to 13%.

The present work is concerned primarily with sources of propellant inefficiency in the PPT to better guide future thruster designs. No conclusions can be made concerning the potential for spacecraft contamination from the exhaust particulates. The PPT used in this work is an inappropriate design for contamination studies because it lacks the housing around the electrodes that a flight unit would certainly have. In addition, the vacuum facility used in the present work is intentionally small to optimize optical diagnostic access, whereas contamination study requires a large chamber to minimize wall interaction. A contamination study for the PPT was performed using a flight-qualified LES 8/9 PPT in a chamber appropriate for this research.[7] No measurable deposition was observed in the backflow region of the thruster, indicating that contamination is not a major concern for these devices. Although the PPT has been shown to not contaminate its own spacecraft significantly, flight missions have been planned using the PPT for precision positioning of multiple satellites flying in formation.[8] In this situation, the PPT from one satellite will at times be firing in the direction of a neighboring satellite, thus increasing the potential for significant contamination. The present work provides estimates of the particle flux and particle size distributions to help mission planners in estimating this contamination potential.

The presence of Teflon particulates in a PPT exhaust was first reported in a 1979 contamination study using the Millipound PPT (150-J discharge energy).[9] This work used SEM/EDAX analysis to conclude that the particulates were composed of the Teflon propellant material. Using the lower-

Received Sept. 20, 1996; revision received Jan. 13, 1998; accepted for publication Feb. 16, 1998.

*Group Leader, Propulsion Directorate. Electric Propulsion Laboratory. Member AIAA.
†Research Engineer, Propulsion Directorate. Member AIAA.
‡Chief, Propulsion Directorate, Spacecraft Propulsion Branch. Member AIAA.

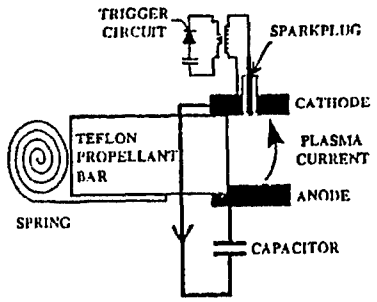

Fig. 1 Schematic of a PPT.

energy LES 8/9 class PPTs (20-J discharge energy), the presence of particulates in the PPT exhaust was again reported by two groups in 1996.[5,7] The first group examined the particulates as a propellant loss mechanism with rough estimates of the particulate mass loss during the initial transient phase when the PPT is first energized.[5,10] The second group noted the presence of the particulates in conjunction with PPT contamination studies.[7] The present work differs from the previous studies by 1) estimating the significance of the particulate mass as a propellant loss mechanism, 2) only collecting particulates after the PPT has achieved steady-state operation, and 3) quantifying the size distribution and spatial distribution that will aid in assessing the contamination potential for nearby satellites.

II. Experimental Apparatus

The experiments are performed in Chamber 5 of the AFRL Electric Propulsion Laboratory.[5] The chamber is 1.2 m in diameter and 1.8 m in length. Typical base pressures of 3×10^{-5} torr are achieved using a turbomolecular pump (1400 l/s) backed by a rotary mechanical pump (1420 l/m).

The experiments are performed on the exhaust from XPPT-1 (Experimental Pulsed Plasma Thruster #1).[5] The XPPT-1, shown in Fig. 2, is similar to the LES 8/9 PPT[11] electrically and geometrically; however, diagnostic access has been maximized in the XPPT-1 design. Following are the major differences between the two designs.

1) The 30-deg thrust angle in the LES 8/9 has been eliminated in XPPT-1.

2) The housing around the electrodes and in the LES 8/9 has been removed in the XPPT-1 design.

3) XPPT-1 is energized using laboratory power supplies.

4) The outer surfaces of the electrodes are covered in the LES 8/9 design.

5) Both electrodes in the XPPT-1 are fabricated from 304 stainless steel compared to the Mallory 1000 (thoriated tungsten) and 17-4 stainless steel used for the LES 8/9 cathode and anode, respectively.

The thruster is designed so that a range of capacitances can be easily tested; however 20 μF was used for all of the present tests, approximately equal to the 17 μF used in the LES 8/9 PPT. Thus, a 1414-V charge is used in the XPPT-1 to simulate the 20-J energy storage of the LES 8/9 charged to 1528 V. The strip line (approximately 50 nH), electrode dimensions (2.5 × 2.5 cm), electrode separation (2.5 cm), fuel-bar geometry (2.5 × 2.5 cm), and spark plugs are identical to those used in LES 8/9. The interface between the energy storage capacitor and the strip line has been modified in XPPT-1 to allow for a Rogowski coil (Ion Physics CM-1-L) that measures the discharge current. This modification adds approximately 70 nH to the circuit inductance.

Broadband light emission from the PPT discharge is digitally recorded using a high-speed framing camera (Stanford Computer Optics 4 QUIK 05). The camera has a minimum 50-ns gate time and an image intensifier for recording low-light signals. The charged coupled device (CCD) array within the camera is 610 × 488 pixels. For the imaging used in the present work this corresponds to a spatial resolution of approximately 150 μm. The camera has only single-frame capability, and so images at different times and shutter speeds are recorded on different PPT discharges.

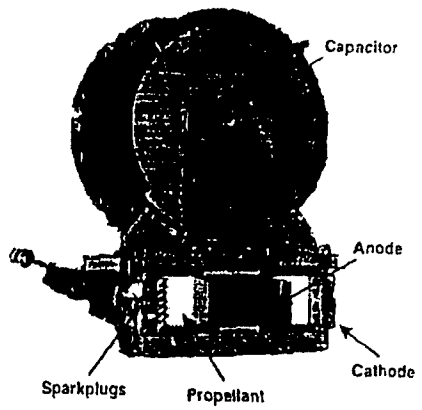

Fig. 2 Photograph of the XPPT-1 PPT with the major components identified.

The witness plates used to collect exhaust samples are disks of 6061-T6 aluminum, 12.7-mm diameter and 3.2-mm thick. The aluminum substrate is chosen because its composition is well known, and its conductivity helps minimize sample charging during SEM/EDAX analysis. Surface analysis was conducted using the facilities of the Jet Propulsion Laboratory Measurement, Test and Engineering Support Division. The principal materials expected in the EDAX analysis are from the Teflon propellant (33% C, 66% F), 304 Stainless Steel electrodes (0.08% C, 69% Fe, 19% Cr, 9% Ni, <2% Mn, and <1% Si), and the 6061-T6 aluminum sample disk (97.9% Al, 1% Mg, 0.6% Si, 0.25% Cr, and 0.25% Cu).

III. Experimental Results

Experiments are performed using XPPT-1 configured with a 20-μF capacitor and charged to 1414 V for a discharge energy of 20 J. The thruster is operated at 1 Hz corresponding to an average power level of 20 W. Prior to the experiment the propellant bar had been discharged over 100,000 times so that a slightly concave shape had been eroded into the front face. During the 6000 discharges of the experiment, the discharge-averaged PPT propellant consumption rate was 24.9 μg/discharge. Although a thrust stand was not used during the present tests, previous measurements indicate that XPPT-1 in this configuration produces approximately 256 μN of thrust.[12] Performance characteristics for XPPT-1 are detailed in Ref. 12.

The 11 witness plates are distributed in arrays oriented parallel and perpendicular to the PPT electrodes, as shown in Fig. 3. All witness plates are located 6 cm from the center of the propellant face. Deposits on the witness plates are accumulated over 1000 PPT discharges. Previous work has shown that when initially energized, the PPT undergoes a transient phase during which the propellant consumption rate increases as the propellant temperature rises.[12] Because this experiment is concerned with understanding the steady-state performance of the PPT, particulate collection during the transient phase was to be avoided. To accomplish this, the witness plates were adhered to a lucite holder that was mounted on an optical translation stage. The holder and plates were placed near the side of the chamber (45 cm from the PPT) and covered with a polyethylene shield. The PPT was energized for the 5000 discharges required to achieve a propellant consumption rate within 5% of the steady-state rate.[12] The PPT was then turned off, the polyethylene shield removed, and the mount containing the sample disks translated into position in front of the PPT. The PPT was re-energized within 60 s, which is insufficient for significant propellant cooling to occur.[12] The removing of the shield and translation of the witness plates was accom

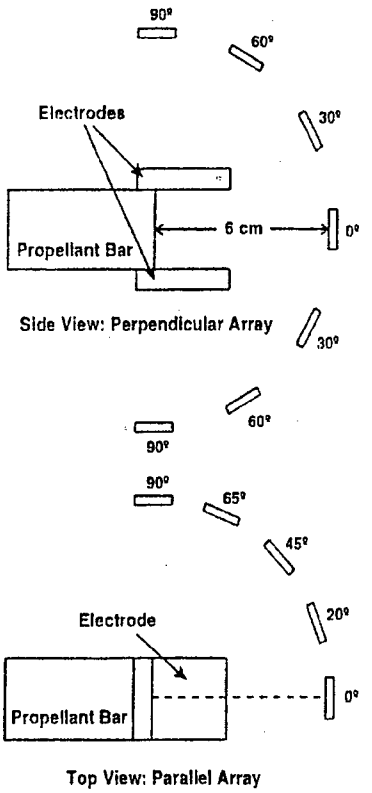

Fig. 3 Locations of the 11 witness plates. Each is positioned 6 cm from the center of the propellant face.

plished using linear–rotary actuators through the chamber walls, without affecting the base vacuum pressure.

Figure 4 shows representative images of the broadband emission from the PPT exhaust. Figure 4a was recorded during the discharge with a 10-μs shutter. The emission is suggestive of a standing arc near the propellant face with streams of plasma accelerated in the thrust direction. The exhaust appears distributed and devoid of particulates. Reduction of the shutter time to 50 ns also shows no evidence of particulates, although the discharge becomes substantially more filamentary. Figure 4b was recorded 100 μs after the discharge with a 10 μs shutter and 14.4 times the light amplification of Fig. 4a. Numerous localized emission sites are apparent. The absence of discharge current at this time, coupled with previous interferometric measurements of a high-density neutral vapor,[5] indicates that the propellant face is continuing to vaporize. Figure 4c is recorded at the same experimental time as Fig. 4b (albeit on different PPT discharges) but with a longer 100-μs shutter and 4.5 times the light amplification of Fig. 4a. Note that the image in Fig. 4c is shown with a reduced scale; however, the spatial resolution is the same as in Figs. 4a and 4b. Large streaks are observed in Fig. 4c, emitted primarily from the electrodes. For the characteristic streak length of 2 cm, a velocity of approximately 200 m/s is inferred. The duration of the streak emission (~100 μs) implies a heat capacity incompatible with a single molecule or plasma motion, implying the higher mass of particulates. The reproducibility of the emission shown in Fig. 4a is quite good. Successive images on different discharges are approximately equal in structure and intensity although minor changes in the arc shape are often observed. The reproducibility of the emission shown in Figs. 4b and 4c is poor, with the number, location, and intensity of the streaks changing dramatically from shot to shot. However, the streaks associated with the particulate emission are apparent on every discharge.

To support the hypothesis of particulates in the PPT exhaust suggested by the broadband emission, the witness plates were exposed to 1000 discharges of the PPT exhaust and analyzed.

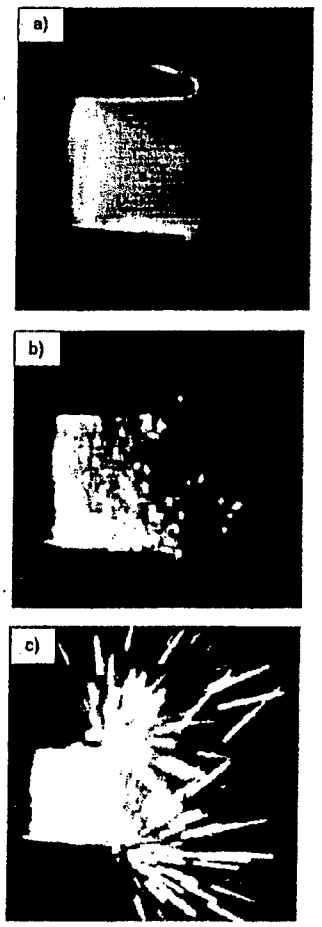

Fig. 4 Broadband emission from the PPT exhaust: a) 1-μs shutter during the PPT discharge, b) 10-μs shutter initiated 100 μs after the discharge, and c) 100-μs shutter initiated 100 μs after the discharge.

The 1000 discharge exposure length was chosen to smooth out the shot-to-shot variations observed in the broadband emission to achieve a shot-averaged particle collection. Examination of the slides using SEM showed a significant population of particulate matter superimposed on a background film. EDAX Spectra was taken of the particulates in an effort to determine whether they originated from the Teflon propellant and should be considered as a propellant loss, as opposed to originating from the steel electrodes. The major finding of the EDAX analysis is that there are two populations of particulates. One population is characterized by a spherical shape, diameters typically 0.3 μm and always less than 1 μm, and strong Fe, Cr and Ni transitions. The second population has more random shape and size, diameters ranging from 200 μm down to less than 1 μm, and a strong F transition. Both populations have strong C transitions as would be expected from either steel or Teflon. The first population is concluded to be steel from the PPT electrodes and the second population is concluded to have originated from the Teflon propellant. The particles from the second population also appear bright in the SEM images which occurs when the electron beam electrically charges the deposit. This indicates that the particles are insulators, unable to conduct excessive charge to the substrate, supporting the conclusion that the second population of particles originated from the Teflon propellant.

The particle size distribution was counted under a microscope for each of the 11 witness plates. Only particles with diameters greater than 25 μm were counted to avoid including the steel particles and because the number of smaller particles was simply too large to be counted manually. The size distribution for the witness plate directly in front of the PPT (θ =

θ deg) is shown in Fig. 5a. Figure 5a shows that the number of particles increases with decreasing size, suggesting that the majority of the particles were probably not counted. Figure 5b shows a histogram of the particle mass estimated from Fig. 5a by assuming that the particles have a radius equal to the average of that range, a volume equal to a half sphere ($V = 2\pi r^3/3$), and the density of Teflon (2152 kg/m^3). Figure 5b shows that the amount of mass in the smaller particle range (25–50 μm) is less than that in the larger particle range (50–75 μm). This suggests that even though the majority of the particles may be of sizes less than 25 μm and weren't counted, the majority of the particulate mass may have been counted. The total particle mass on this witness plate, for sizes greater than 25 μm, calculated by adding the masses in the four groups of Fig. 5b, is 144 ± 18 μg.

Because the number of particles counted in a given range is typically low (<500), the measurement uncertainty is presumed to be dominated by statistical variations in the particle count. The statistical variation in the particle count is estimated as the square root of the number counted, i.e., $\Delta N = N^{1/2}$. The uncertainties in calculated quantities such as total particulate mass are determined solely from the uncertainty in the particle count. Clearly, the greatest source of uncertainty in estimates of the particulate mass lies in the assumption that the volume of the individual particles is that of a half sphere. For the case of spherical particles, this approximation underestimates the particle mass by a factor of 2. For the case of particles that become somewhat flattened out this approximation may underestimate the particle mass by as much as a factor of 2. Determining the measurement uncertainty associated with this approximation would require a three-dimensional imaging of each particle, which was not attempted in the present work. Thus the measurement uncertainty represents an assessment of the random uncertainty in the measurements, but ignores a potential systematic uncertainty associated with the half-sphere approximation.

The spatial distribution of the particulate deposits is shown in Fig. 6 for both the perpendicular (Fig. 6a) and parallel (Fig. 6b) sample arrays. The distributions are calculated by counting the particles on each witness plate and estimating the total particulate mass, as was done earlier for the witness plate at $\theta = 0$ deg. The parallel case is shown with an exponential fit and the perpendicular case is shown with a $\cos^7\theta$ fit.

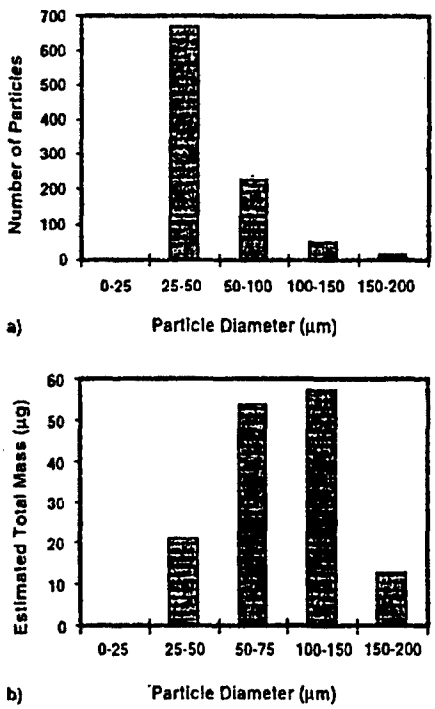

Fig. 5 Histograms of the particulate distribution on the witness plate located at $\theta = 0$: a) Size distribution for three different characteristic diameter ranges, and b) associated mass distribution.

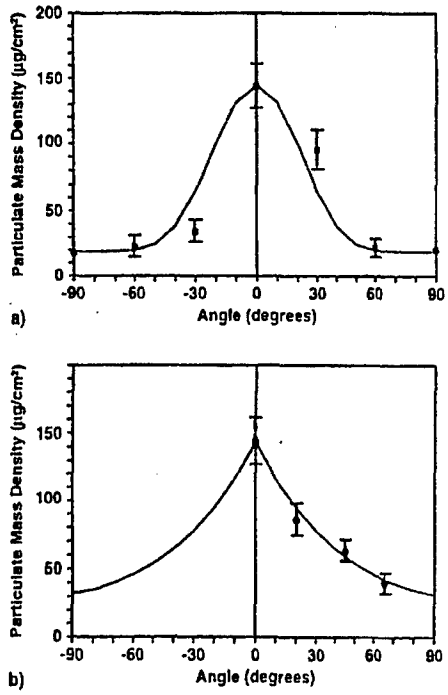

Fig. 6 Spatial distribution of particulate mass on the witness plates: a) The perpendicular distribution is shown with a $\cos^7\theta$ fit, and b) the parallel distribution is shown with an exponential fit.

IV. Discussion

The total particulate mass emitted by the PPT is estimated by integrating the spatial distributions of Fig. 6 over the solid angle in front of the thruster. The integration is complicated by the asymmetric nature of the distributions, as evidenced by the differing fits for the data from the parallel and perpendicular arrays. For the integration over the solid angle, the parallel and perpendicular fits are each used for 90 deg and zero mass deposition is used in the backplane of the thruster. The integration yields a total emitted particulate mass of 9.8 ± 0.7 mg. During the 1000 discharge exposure of the witness plates, this mass averages to a rate of 9.8 ± 0.7 μg/discharge, which is 40 ± 3% of the 24.9-μg/discharge propellant consumption rate measured over the 6000 discharges of the entire experiment.

A previous characterization of transient effects in the PPT propellant consumption rate showed that the propellant consumption rate increases over time as the propellant temperature rises to a steady state.[12] Comparing the particulate mass emitted between discharges 5000 and 6000 to the propellant mass consumed between discharges 0 and 6000 will cause a systematic overestimation of the propellant fraction consumed in the form of particulates. This results from the propellant consumption rate between discharges 5000 and 6000 being systematically higher than the rate averaged from discharge 0 to 6000. At worst case, based on the data of Ref. 12, the propellant consumption rate during the discharges where particulates are collected is 5% higher than the measured rate, which averaged over all 6000 discharges. This effect could lower the propellant mass fraction consumed by particulates to 37%. Because this is within the uncertainty of the 40 ± 3% mass fraction, and an instantaneous propellant consumption measurement to fully quantify this effect is presently not possible in PPT experiments, the higher value will be used.

The particulate emission is expected to contribute minimally to the total PPT thrust. If the emission was uniformly directed along the thrust vector, the 9.8 μg/discharge of particulates at

200 m/s would produce 2 μN, less than 1% of the total thrust. Based on Fig. 4c, the particulate emission is closer to omnidirectional, indicating that the 2-μN contribution is a liberal estimate. If the propellant consumption rate can be decreased by eliminating the particulate emission, without affecting the thrust, then the PPT thrust efficiency increases. For a 40% propellant mass reduction

$$\frac{\Delta\eta}{\eta} = \frac{T^2/2f(0.6\ m)P}{T^2/2\ fmP} = 1.7$$

which for a LES 8/9 PPT[11] implies that the thrust efficiency would increase from 7.9 to 13%. This estimate shows the magnitude of the propellant savings and associated improvement in efficiency achievable in the ideal case where modifications to the thruster enable the particulate mass to be recovered without reducing the thrust. In practice, the energy associated with creating and accelerating the particles has to be deposited somewhere. This free energy may cause other changes to the PPT discharge that result in small or negligible changes in efficiency.

Understanding the mechanism behind the creation of the particulates is critical to eventually minimizing this propellant loss. A possible mechanism is that particle formation results from a high-pressure vapor created below the Teflon surface. Radiative energy from the discharge arc deposits beneath the propellant face, either heating trapped gases or contributing to the vaporization of small amounts of solid propellant. The embedded heated vapor would create high gas pressures that explosively eject the particulates. Similar effects have been observed in related work on ablation-controlled arcs.[13] In this scenario, propellant modifications that decrease the radiative energy transport may reduce the particulate emission. Also, changing to a cast polymer may reduce the particulate emission by reducing the volume of gasses trapped in the propellant.

Emission streaks in Fig. 4c imply that a majority of the particles originate from the electrodes. Two possible interpretations of this observation are offered. First, the streaks in Fig. 4c are due to the emission of steel particles from the electrodes and are essentially unrelated to the propellant losses. This would seem to be the most likely case because steel particles were detected in the EDAX analysis, and because the higher temperature of molten steel (T_{melt} = 1427°C) as compared to Teflon (T_{melt} = 327°C) increases the emission intensity within the detectable sensitivity range of the camera (approximately 300–600 nm). In this scenario, the particulate streaks may be reduced by changing the electrode material, but this would not be expected to have a significant effect on the particulate propellant losses.

Second, the streaks may be a result of vapor from previous discharges condensing on the electrode surface. Localized heating from the plasma arc then raises the electrode temperature above the vaporization temperature of the coating. Some coating material is vaporized near the electrode surface creating a high gas pressure layer between the electrode and the solid coating. The remaining solid is then gasdynamically accelerated from the electrode in the form of particulates. This scenario would seem impractical for a uniform Teflon coating, because the electrical insulation properties of Teflon could prevent the arc conduction. To be feasible, either the coating would have to be conductive or nonuniform. The coating could be conductive if it were comprised of Teflon derivatives such as carbon. A nonuniform coating would enable the arc to conduct near a coated region, heating the steel electrode above the coating vaporization temperature. The heat could then thermally conduct beneath the nearby coating causing the subsequent vaporization and ejection. In this scenario, the particulate emission is a direct result of late-time vaporization, and modifications that minimize the vaporization may also reduce the particulate emission. One method of accomplishing this reduction has been suggested in experiments that show that reducing the PPT propellant temperature may reduce the late-time vaporization.[12]

The emission images imply that particulate ejection from the electrodes occurs well after the discharge with no detectable particulates during the PPT discharge. This may actually result from the relatively strong emission from the plasma arc overwhelming the weaker emission from the particulates. The broadband emission image 100 μs after the discharge when particulates are apparent (Fig. 4b) was obtained with 14.4 times the image intensification as the image during the discharge (Fig. 4a). It is also important to note that the streaks apparent in Fig. 4c may not be associated with the particulate deposits on the witness plates. The propellant particles may be emitted at low temperature with a low light emission level in the spectral range of the camera and, therefore, never be observable.

V. Summary and Conclusions

Surface analysis on exhaust deposits from the PPT reveal a significant quantity of propellant material in particulate form. Estimates of the total mass exhausted in this form show that particulates may account for 40 ± 3% of the total propellant usage, indicating that this is a significant, and possibly the dominant, source of propellant inefficiency in these devices.

One source of the particulates is believed to be energy deposition below the Teflon surface. This energy vaporizes material or heats trapped vapors, creating a high gas pressure behind the propellant face that ejects particulate material. A second potential source of ejected particles results from vaporized Teflon propellant condensing on the electrode surfaces. During subsequent PPT discharges, vaporization beneath the coating ejects the Teflon material as particulates. PPT modifications that reduce the energy transmission into the propellant or decrease the late-time vaporization are expected to decrease the propellant losses associated with particulate emission.

Research directed toward minimizing the particle ejection can have a significant impact on PPT thrust efficiency. Recovering the propellant consumed in the form of particulate emission with no decrease in thrust would increase the PPT thrust efficiency by a factor of 1.7. In the case of a LES 8/9 PPT[11] this would increase the efficiency from 7.9 to 13%.

Acknowledgments

Jason Lotspeich was supported by the U.S. Air Force Office of Scientific Research. The authors acknowledge the assistance of Jim Kullick of the Jet Propulsion Laboratory for his assistance in performing the SEM/EDAX analysis.

References

[1]Guman, W. J., and Nathanson, D. M., "Pulsed Plasma Microthruster for Synchronous Orbit Satellite," *Journal of Spacecraft and Rockets*, Vol. 7, No. 4, 1970, pp. 409–415.

[2]Brill, Y., Eisner, A., and Osborn, L., "The Flight Application of a Pulsed Plasma Microthruster; the NOVA Satellite," AIAA Paper 82-1956, Nov. 1982.

[3]Guman, W. J., and Williams, T. E., "Pulsed Plasma Microthruster for Synchronous Meteorological Satellite (SMS)," AIAA Paper 73-1066, Oct. 1973.

[4]Vondra, R. J., "The MIT Lincoln Laboratory Pulsed Plasma Thruster," AIAA Paper 76-998, Nov. 1976.

[5]Spanjers, G. G., McFall, K. A., Gulczinski, F. S., III, and Spores, R. A., "Investigation of Propellant Inefficiencies in a Pulsed Plasma Thruster," AIAA Paper 96-2723, July 1996.

[6]Solbes, A., and Vondra, R. J., "Performance Study of a Solid Fuel Pulsed Electric Microthruster," *Journal of Spacecraft*, Vol. 10, No. 6, 1973, pp. 406–410.

[7]Myers, R. M., Arrington, L. A., Pencil, E. J., Carter, J., Heminger, J., and Gatsonis, N., "Pulsed Plasma Thruster Contamination," AIAA Paper 96-2729, July 1996.

[8]Blandino, J. J., Cassady, R. J., and Peterson, T. T., "Pulsed Plasma Thrusters for the New Millenium Interferometer (DS-3) Mission," International Electric Propulsion Conf., Paper 97-192, Aug. 1997.

[9]Rudolph, L. K., and Jones, R. M., "Pulsed Plasma Thruster Contamination Studies," International Electric Propulsion Conf., Paper 79-2106, Oct. 1979.

[10]Spanjers, G. G., Lotspeich, J. S., McFall, K. A., and Spores, R. A., "Propellant Inefficiency Resulting from Particulate Ejection in a Pulsed Plasma Thruster," Space Technology and Applications International Forum (STAIF-97), Albuquerque, NM, Jan. 1997; *American Institute of Physics Conference Proceeding 387*, edited by Mohamed S. El-Genk, American Inst. of Physics Press, Woodbury, NY, 1997, p. 323.

[11]Vondra, R. J., and Thomassen, K. I., "Flight Qualified Pulsed Electric Thruster for Satellite Control," *Journal of Spacecraft and Rockets*, Vol. 11, No. 9, 1974, pp. 613–617.

[12]Spanjers, G. G., Malak, J. B., Leiweke, R. J., and Spores, R. A., "The Effect of Propellant Temperature on Efficiency in the Pulsed Plasma Thruster," AIAA Paper 97-2920, July 1997.

[13]Ruchti, C. B., and Niemeyer, L., "Ablation Controlled Arcs," *IEEE Transactions on Plasma Science*, Vol. PS-14, No. 4, 1986, pp. 423–434.